

## The Study of Micro- and Nanostructure of Interlayer Cleavage Surfaces of InSe Layered Crystals Intercalated with Nickel

P.V. Galiy<sup>1,\*</sup>, P. Mazur<sup>2</sup>, A. Ciszewski<sup>2</sup>, I.R. Yarovets<sup>1</sup>, T.M. Nenchuk<sup>1</sup>, Frank Simon<sup>3</sup>,  
Ya.M. Buzhuk<sup>1</sup>, V.L. Fomenko<sup>1</sup>

<sup>1</sup> Ivan Franko Lviv National University, 50, Dragomanov St., 79005 Lviv, Ukraine

<sup>2</sup> Institute of Experimental Physics, University of Wrocław, 9, Max Born Pl., 50-204 Wrocław, Poland

<sup>3</sup> Leibniz Institute of Polymer Research Dresden, P. O. Box 120 411, D-01005 Dresden, Germany

(Received 06 November 2015; published online 15 March 2016)

This paper presents the results of experimental study concerning elemental-phase composition, crystallographic structure, topography and electron-energy structure of interlayer cleavage surfaces (0001) obtained for nickel intercalated ( $\text{Ni}_{3d}\text{InSe}$  intercalate) InSe layered crystals, by means of qualitative and quantitative X-ray photoelectron spectroscopy (XPS), low-energy electron diffraction (LEED), and scanning tunneling microscopy/spectroscopy (STM/STS). It was established that for all layered crystals' intercalates with different concentrations of nickel in initial synthesized  $\text{InSe} + x$  at.% Ni ( $x \leq 10.0$  %) alloys and layered crystals further grown from them by Bridgman-Stockbarger method and subjected to intercalation, the maximum concentration of nickel on the cleavage (0001) surfaces of  $\text{Ni}_x\text{InSe}$  intercalates and, accordingly, in the interlayer gaps of up to 7.67 at. % is observed at 0.75 at. % of nickel in synthesized alloys. Nickel does not interact with selenium and indium and there is also no interaction with oxygen and carbon. It is established that nickel is placed in the interlayer gaps of  $\text{Ni}_x\text{InSe}$  intercalates and, accordingly, appears on the interlayer cleavage (0001) surfaces as fine-phase metal nickel clusters. The studied  $\text{Ni}_x\text{InSe}$  intercalate system is the perfect hybrid structure with the ability to use in magnetoelectronics.

Keywords: Layered crystals, Interlayer cleavage surfaces, X-ray photoelectron spectroscopy, Elemental-phase composition, Topography, Atomic structure, Scanning tunneling microscopy, Scanning tunneling spectroscopy, Low energy electron diffraction.

DOI: [10.21272/jnep.8\(1\).01012](https://doi.org/10.21272/jnep.8(1).01012)

PACS numbers: 82.80.Pv, 68.47.Fg, 61.46.\_w, 68.37.Ef, 68.37.Ps, 68.47.Fg, 61.05.Jh

### 1. INTRODUCTION

One of the features of semiconductor layered crystals (LC), to which InSe belongs, is the presence of the van der Waals gap between the layers that makes it possible to introduce into the interlayer space of the crystals (by intercalation method) atoms of other substances, for example, 3d-atoms of metals of the iron group, in particular, nickel, chromium, etc. [1].

Such hybrid  $\text{InSe}(\text{Me})$  structures obtained based on InSe LC (Fig. 1a, b), which are also called the  $\text{Me}_{3d}\text{InSe}$  intercalates, are new materials [2] and should be a system of "plane" nanostructures formed by magnetic impurities of 3d-atoms of metals disposed in the van der Waals gaps of a layered semiconductor InSe crystal (Fig. 1b).

The technique of intercalation of LC in the growth process by the Bridgman method in evacuated quartz ampoules and subsequent thermal treatments of the obtained  $\text{Ni}_{3d}\text{InSe}$  samples as well as structural studies of the prepared intercalates allow to state, as the authors of [3, 4] assume, about the disposition of  $\text{Ni}_{3d}$  magnetic intercalate only in the van der Waals gap, but for the limited nickel concentrations. Alternation of magnetic nanolayers with four diatomic Se-In, In-Se layers of the semiconductor InSe sandwich allows to avoid coagulations of these nanolayers along the anisotropy axis  $c$  (Fig. 1a). However, there is a possibility of coagulation of magnetic atoms of the intercalate inside the van der Waals gap with the formation of clusters.

Therefore, the aim of our work was to perform the so-called direct studies of the elemental-phase composition,

micro- and nanostructure of interlayer cleavage surfaces (CS) (0001) of  $\text{Ni}_{3d}\text{InSe}$  intercalates. Such investigations should give a direct answer about the presence/absence of nickel and its amount; its phase composition at the interlayer cleavage surfaces and thus the quality of the obtained hybrid structures in whole and prospects of their application in  $\text{Ni}_{3d}$  intercalation during the growth with further processing. This is important, taking into account that the method of electrochemical intercalation with the application of an electric field and movement of intercalating nickel ions in the intercalate is more complicated.

Intercalation formation of nanosystems [1, 3, 4] has a number of significant advantages over other methods of overcoming coagulation and agglomeration processes in order to create materials for spintronics [2, 5], nanophotonics [6], in which semiconductor layers alternate with layers of other substances, which can have another nature. Today, this technique provides the formation at the atomic-molecular level of nanostructures of functional micro-, nanoelectronics; and creation of whole functional microblocks with "output" to the macro-functional devices is possible in the future [3]. Therefore, the study of the  $\text{Me}_{3d}\text{InSe}$  intercalates, as well as  $\text{Ni}_{3d}\text{InSe}$  in particular, is under constant attention of researchers [6-8].

### 2. OBJECTS OF STUDY

The crystals of  $\text{Ni}_{3d}\text{InSe}$  intercalates with different initial discrete atomic nickel concentrations were obtained as follows. The synthesis of  $\text{Ni}_x\text{InSe}$  ( $x = 0; 0.5; 0.75$ ;

\*[galiy@electronics.lnu.edu.ua](mailto:galiy@electronics.lnu.edu.ua)

1.0; 2.0; 10.0 wt. % of Ni) compounds, from which the InSe(Ni) LC were grown, was carried out by the direct synthesis of the alloy of initial components (In, Se, Ni) in quartz ampoules evacuated to the residual gas pressure of  $10^{-3}$  torr. Vibration mixing was used in order to homogenize the alloy. Substances of the mark "HPM" were taken as the initial components. The synthesis was conducted during three days at a temperature not higher than 960 K to prevent the formation of nickel selenide compounds. Single crystals of layered  $Ni_xInSe$  intercalates were grown by the Bridgman-Stockbarger method [4, 7] in evacuated quartz ampoules from the synthesized  $InSe + x$ wt. % of Ni ( $x \leq 10$  %) alloys. The grown LC were heat-treated in evacuated quartz ampoules at the temperature of 870 K during 60 hours for the uniform distribution of Ni impurity in the layered single crystal and acceleration of the process of its shift into the interlayer gaps (intercalation with nickel) (Fig. 1a, b) [7].

The X-ray structural and phase analysis using diffractometer DRON-4-07 ( $CuK_{\alpha}$ -radiation) was performed to study the structure and phase composition of the obtained single crystals of layered  $Ni_xInSe$  intercalates. The diffraction patterns of pure initial  $Ni_xInSe$  intercalate ( $x = 0$ , pure InSe LC) and  $Ni_xInSe$  ( $x \neq 0$ ) intercalated with different nickel concentration are indexed in the trigonal system (rhombohedral structure,  $\gamma$ -polytype),  $R3m$  ( $C_{3V}^5$ ) space group (Fig. 1a, b). The X-ray phase analysis, as an integral research method of the LC volume, showed that the obtained  $Ni_xInSe$  intercalate is homogeneous. Substitution phases of nickel selenide compounds as well as free nickel were not revealed [4]. The absence of the X-diffraction peaks (when studying the LC volume), which correspond to metal nickel, also confirms the integral homogeneity of the obtained crystalline  $Ni_xInSe$  intercalate. Although, as our further studies of interlayer CS of InSe LC intercalated with nickel ((0001) CS of  $Ni_xInSe$  LC) show, the situation is somewhat different in a nano-scale. The results of these studies obtained by the corresponding surface-sensitive methods will be given below.

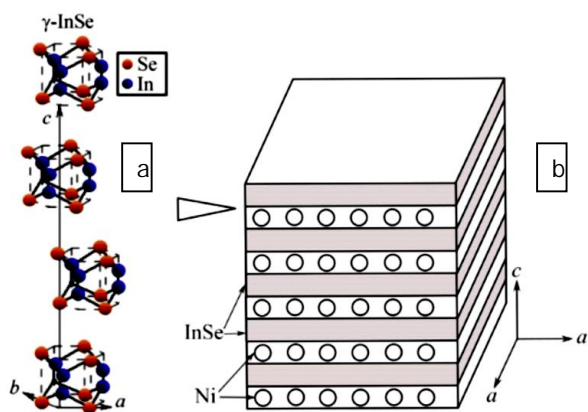


Fig. 1 – Structure of  $\gamma$ -InSe LC (a) and schematic representation of  $Ni_xInSe$  hybrid structure (intercalate) (b). a) Crystal structure of  $\gamma$ -InSe LC. Lattice constants are given by the data of work [9]:  $a = b = 4.002$  Å,  $c = 24.946$  Å ( $R3m$  ( $C_{3V}^5$ ) space group). b) Schematic representation of  $Ni_xInSe$  hybrid structure, in which 3d atoms of nickel (Ni) are located in the interlayer gaps of the LC (between covalently bound (into the semiconductor layers) InSe atoms. The triangle in the left upper part of the figure indicates the cleavage direction with obtaining (0001)  $Ni_xInSe$  LC

To obtain (0001) CS of pure  $\gamma$ -InSe LC and intercalated  $Ni_xInSe$ , the samples of a special shape (pedestal) of the size of  $3 \times 6 \times 4$  mm<sup>3</sup> were cleaved at 295 K by a steel needle. Methods of electron spectroscopy and microscopy, which are extremely informative, now occupy a leading place among the effective methods of studying the material surface. The elemental-phase composition of the surface belongs to the main microscopic characteristics, in addition to crystallography, topography and electron-energy structure; therefore, the study of interlayer (0001) CS of  $Ni_xInSe$  intercalates is the main task in our case. Thus, a question on the presence or absence of 3d Ni atoms and in what phase (disperse "cluster" or completely formed metal phase) and in what quantities are they located at the interlayer (0001) CS of  $Ni_xInSe$  intercalates is a key one.

Therefore, we present here the results of experimental study of the elemental-phase composition of (0001) CS of pure InSe LC and their  $Ni_xInSe$  intercalates obtained by X-ray photoelectron spectroscopy (XPS), low-energy electron diffraction (LEED) as well as scanning tunneling microscopy/spectroscopy (STM/STS).

### 3. RESULTS AND DISCUSSION

#### 3.1 Elemental-phase composition of (0001) CS of $Ni_xInSe$ intercalates

The investigation of the elemental-phase composition of (0001) CS of pure InSe LC and their  $Ni_xInSe$  intercalates ( $x = 0; 0.5; 0.75; 1.0; 2.0$  wt. %) was performed by the XPS method. The surfaces under investigation were obtained by cleavage of the LC in air; therefore, during a short period of time (2-15 min) they were in contact with the atmosphere:  $N_2$ ,  $O_2$ ,  $CO_2$ ,  $H_2O$ ,  $CH_x$  before transportation to the ultra-high vacuum (UHV) ( $10^{-9}$  torr) measuring XPS chamber.

The XPS spectra are obtained using the device AXIS ULTRA (by Kratos Analytical, England), in which we utilized monochromatic X-rays  $AlK_{\alpha}$  ( $h\nu = 1486.6$  eV) with the energy line width at half-height of the maximum (WHH) equal to 0.3 eV. The source of X-rays with  $Al$ -anticathode operated in the mode with  $I = 20$  mA and  $U = 15$  kV. The XPS spectra were recorded at the residual gas pressure in the spectrometer chamber of  $10^{-9}$  torr. The photoelectrons of chemical elements excited by X-rays, emitted at the angle of  $90^\circ$  to the surface entered a hemispherical energy analyzer. The XPS spectrometer for the determination of the binding energies of chemical elements was calibrated using Ag  $3d_{5/2}$  line of energy of 368.2 eV with WHH of 1.7 eV. The relative energy separation of the energy analyzer of emitted electrons is 1.5%.

Scanning of the energy analyzer for the determination of the kinetic energies of emitted electrons and, thus, elucidation of the binding energies and identification of the chemical elements were carried out in the range of 10-1100 eV (wide energy window of panoramic scanning). The analyzer used the energy window of 210 eV – panoramic (with the energy increment of 200-300 meV) and the window of 20-30 eV (with the energy increment of 20-30 meV) for precision scanning and determination of the binding energies of chemical elements (Se  $3d_{5/2+3/2}$ , C 1s, N 1s, In  $3d_{5/2+3/2}$ , O 1s, Ni  $2p_{3/2}$ ) and the shape of their peaks (detection of chemical shifts) for the purpose of phase analysis (appearance of new electronic interactions at (0001) CS of  $Ni_xInSe$  intercalates).

The XPS spectra are obtained by the hemispherical energy analyzer. The spectral data were output to the counter rate meter and fed to a PC through an interface. Execution of repeated precision energy scanning, data accumulation and processing by software results in the improvement of the signal/noise ratio and achievement of energy separation in the spectrum  $\Delta E \cong 0.025-0.03$  eV. This, in whole, provides the quality improvement of the XPS spectra, realization of their background correction by software and more precise determination of the binding energy of the "peaks" and peak area for the observed chemical elements. The peak area of chemical elements is used for the quantitative determination of the relative elemental composition of (0001) CS of  $\text{Ni}_x\text{InSe}$  LC intercalates and possible formation on them (when cleaving in air) of the interface layers with the participation of the main chemical elements, such as In, Se, Ni, and atmospheric gases as  $\text{N}_2$ ,  $\text{O}_2$ ,  $\text{CO}_2$ ,  $\text{H}_2\text{O}$ , and  $\text{CH}_x$ .

The shape of the experimental peaks, their decomposition into components, and binding energy can vary due to changes in chemical interactions of elements at the interlayer (0001) CS of  $\text{Ni}_x\text{InSe}$  LC intercalates with the formation of new phases in the interfaces. Thus, XPS studies give information on the elemental-phase composition of the interface layers formed on (0001) CS of the LC.

The panoramic XPS spectrum of (0001) CS of  $\text{Ni}_x\text{InSe}$  intercalates is illustrated in Fig. 2. The peaks of carbon, oxygen, nitrogen (C 1s, O 1s, N 1s) are also observed in the XPS spectrum of (0001) CS except the present main

reference peaks of the components of  $\text{Ni}_x\text{InSe}$  LC intercalate (Se 3d, In 3d<sub>5/2</sub>, In 3d<sub>3/2</sub>, Ni 2p<sub>3/2</sub>). The latter is the result of absorption of the atmospheric components on (0001) CS of  $\text{Ni}_x\text{InSe}$  intercalates when they are cleaved in air. Moreover, the relaxation peaks of the Auger electrons of Se LMM, In MNN, and O KLL are present. The similar situation was observed in the works [10, 11] for (100) CS of  $\text{In}_4\text{Se}_3$  LC.

The most intense XPS peaks are Se 3d<sub>5/2</sub> + 3/2, In 3d<sub>5/2</sub>, In 3d<sub>3/2</sub>, Ni 2p<sub>3/2</sub>, C 1s, O 1s, which, like all others, were identified using the database [12] and recorded on the precision scale of "binding energies" in order to estimate the manifestation of new chemical interactions with the electron charge transfer to the (0001) CS of  $\text{Ni}_x\text{InSe}$  LC intercalates and in their interface layers. The control of possible CS charging under X-irradiation and record of the XPS spectra was necessary, since it influences the XPS results (obtained binding energies of chemical elements), therefore, the binding energies of elements were corrected with respect to C 1s-peak of carbon (284.5 eV).

For precision expanded scanning and more exact determination of the binding energies of chemical elements (Se 3d<sub>5/2</sub> + 3/2, In 3d<sub>5/2</sub>, In 3d<sub>3/2</sub>, Ni 2p<sub>3/2</sub>) and the shape of their peaks (detection of chemical shifts) for the purpose of phase analysis (appearance of new electronic interactions at (0001) CS of  $\text{Ni}_x\text{InSe}$  intercalates and in their interface layers), the analyzer used the energy window of 20-30 eV with the energy increment of 20-30 meV (see Fig. 3, Fig. 4, Fig. 5).

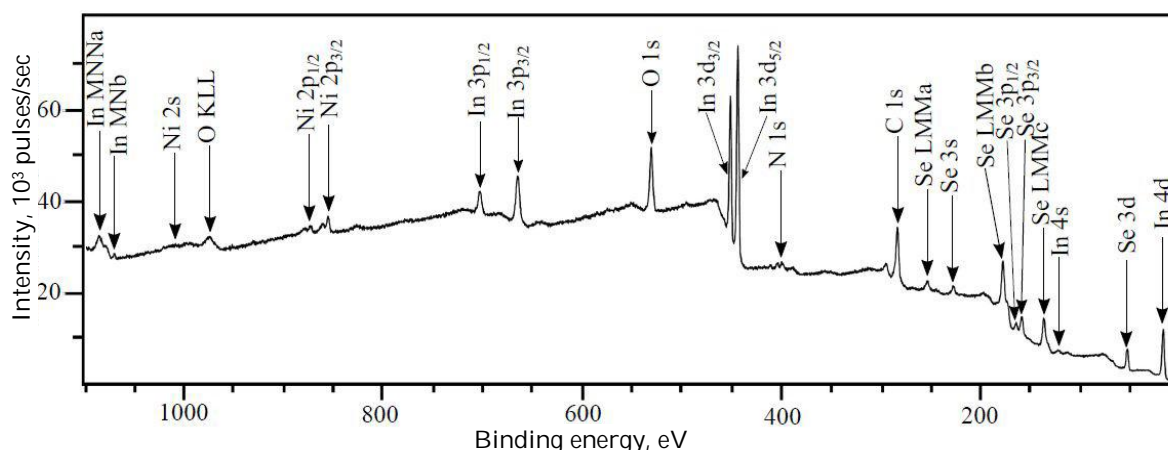


Fig. 2 – Panoramic spectrum (10-1100 eV) of (0001) CS of  $\text{Ni}_x\text{InSe}$  LC intercalates without background correction of the peak intensity of chemical elements at Ni concentration of  $x = 0.75$  wt. % in the initial  $\text{Ni}_x\text{InSe}$  alloy used to obtain the single crystal

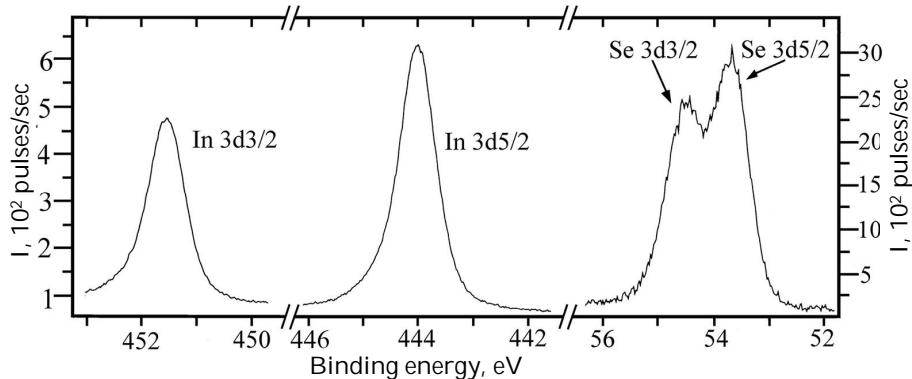


Fig. 3 – Expanded XPS spectra of the components (Se 3d<sub>3/2</sub>; Se 3d<sub>5/2</sub>; In 3d<sub>3/2</sub>; In 3d<sub>5/2</sub>) for fresh (0001) CS of  $\text{Ni}_x\text{InSe}$  intercalates (short exposure time in air after cleaving is 2-15 min)

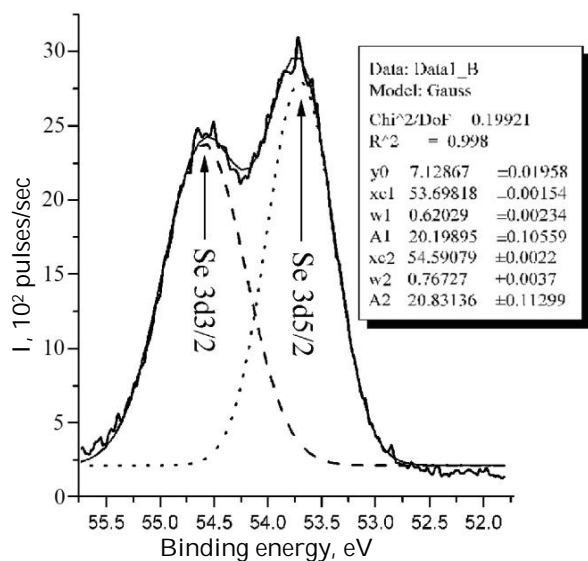


Fig. 4 – Fragment of “expanded XPS spectrum” of Se doublet peak for fresh (0001) CS of Ni<sub>x</sub>InSe intercalates and its decomposition into individual Gaussians with background correction

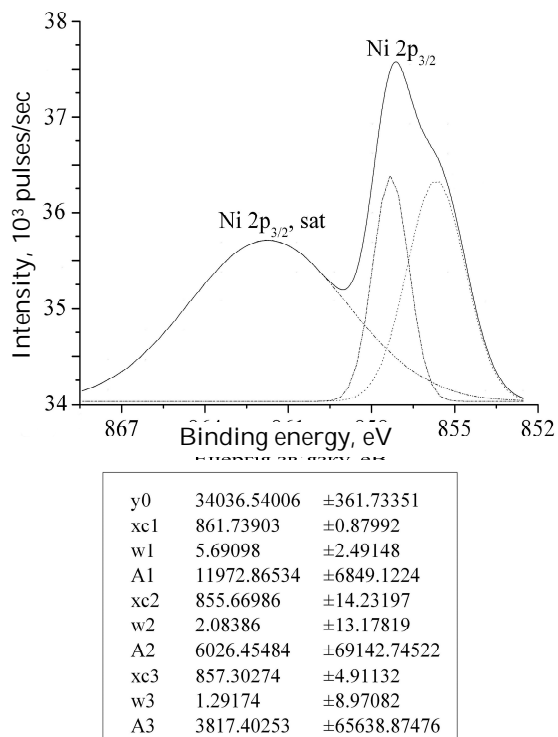


Fig. 5 – Decomposition of the peak Ni 2p<sub>3/2</sub> into two Gaussians in the package Origin 7.5. Software chooses: y<sub>0</sub> – background level; x<sub>c</sub> – centers of the peaks (Gaussians) – binding energies; w – half-height widths of the peaks and calculates the area (A) under each Gaussian (see Table 1)

The exact energy positions of the peaks, which we are interested in, namely XPS peaks Se 3d<sub>5/2</sub> + 3/2, In 3d<sub>5/2</sub>, In 3d<sub>3/2</sub>, Ni 2p<sub>3/2</sub> recorded on the expanded precision scale of binding energies are illustrated in Fig. 3. Each case of analysis of the XPS peak shape with the decomposition into components by Gaussians is carried out using the software Origin 7.5 with the background correction and determination of the energy position of the peak (binding energies of electrons of chemical elements) with the

control of the XPS database [12] and area under the peak (see Fig. 4).

It is important to elucidate in what electronic (chemical) interactions there is nickel, which is localized in the interlayer gaps of Ni<sub>x</sub>InSe intercalates and, when they are cleaved along the interlayer gaps, appears on (0001) CS of the intercalates.

As a result of the processing of the XPS spectra of (0001) CS of Ni<sub>x</sub>InSe intercalates, analyzing the doublet peaks of indium (In 3d<sub>3/2</sub>; In 3d<sub>5/2</sub>) (Fig. 3) and selenium (Se 3d<sub>3/2</sub>; Se 3d<sub>5/2</sub>) (Fig. 3 and Fig. 4) relative their binding energies and shape (structure), it is established that for fresh (0001) CS and, correspondingly, in the interlayer gaps, interactions between nickel and indium and between nickel and selenium are absent.

Background correction of the peak intensities of chemical elements, determination of the binding energies and peak “intensity” of the element in the presence of doublets with overlapping of intensities of individual peaks, as, for example, in the case of Se 3d<sub>5/2</sub> + 3/2 (Fig. 4), appearance of new chemical interactions with varying shape and energy position, are conducted using the software Origin 7.5 with the decomposition of complex (in shape) peaks (Fig. 4) into elementary Gaussians (1)

$$y = y_0 + \frac{A}{w \times \sqrt{\pi/2}} \times \exp\left(-2 \left(\frac{x - x_c}{w}\right)^2\right), \quad (1)$$

where y<sub>0</sub> is the background level; x<sub>c</sub> are the centers of the peaks (Gaussians) – binding energies; w are the half-height widths of the peaks; A is the peak (Gaussian) area – peak “intensity” of the chemical element. This decomposition procedure of “complex peaks of chemical elements” into components with obtaining reference (main elementary peaks of chemical elements) minus the background (background correction) is necessary for the quantitative XPS of (0001) CS of Ni<sub>x</sub>InSe intercalates by the pure standards method.

Based on the analysis of the experimental XPS peaks of nickel (Ni 2p<sub>3/2</sub>) (see Fig. 2 and Fig. 5), as well as the binding energies of nickel electrons given in the databases [12] when it belongs to different possible compounds, according to the conditions of our experiments, one can assume that nickel can interact, mainly, with oxygen “forming Ni-O bonds” and water vapor (Ni-H<sub>2</sub>O interaction) “forming Ni(OH)<sub>2</sub>” (Table 1). The last interactions at (0001) CS of Ni<sub>x</sub>InSe intercalates are impossible at room temperatures.

Therefore, as it was shown by the decompositions of the reference peaks of nickel Ni 2p<sub>3/2</sub>, oxygen O 1s, and carbon C 1s and by the analysis of the doublet peaks of selenium Se 3d<sub>5/2</sub> + 3/2 and indium In 3d<sub>3/2</sub> + 5/2, we managed to find out that nickel, which was in the interlayer gaps of Ni<sub>x</sub>InSe (x = 0; 0.5; 0.75; 1.0; 2.0 wt. %) intercalates and, correspondingly, at the interlayer (0001) CS, does not interact with selenium and indium, as well as the interactions with oxygen and carbon are absent (see Fig. 3, Fig. 4, Fig. 5, and Table 1). Nickel is, to a greater extent, a finely dispersed phase of metal nickel clusters that is confirmed by the results obtained by STM/STS and LEED methods presented in our work [13].

The results of the analysis of the binding energies of the reference peaks in the XPS spectra of (0001) CS of

Ni<sub>x</sub>InSe intercalates and their interface Ni<sub>x</sub>InSe (O, C) layers with the binding energies for chemical elements, which form them, presented in the available databases, when chemical elements In, Se, Ni enter different possible, for our case, compounds, are given in Table 1.

The results of the work [4] indicate the features of the change in the magnetic susceptibility of Ni<sub>x</sub>InSe LC intercalates intercalated with magnetic impurities of 3d nickel atoms located in the van der Waals gaps depending on their concentration. The quantitative characteristics as for the nickel location at (0001) CS of Ni<sub>x</sub>InSe intercalates can be obtained using the XPS experimental results by the pure standards method described in the works [10, 11, 14].

Table 1 – Results of the analysis of the reference peaks in the XPS spectra of (0001) CS of Ni<sub>x</sub>InSe intercalates and their interface layers

	Reference peak	Compound: electronic interactions and binding energy, eV	
(0001) CS of Ni <sub>x</sub> InSe	In 3d <sub>5/2</sub>	Ni <sub>x</sub> InSe	444.00
	Se 3d <sub>5/2</sub>		53.70
	Ni 2p <sub>3/2</sub>	Ni <sub>x</sub> InSe	857.30 (Ni-O)
			855.67 (Ni-H <sub>2</sub> O)
	C 1s	Ni <sub>x</sub> InSe	283.70
O 1s <sub>1/2</sub>	Ni <sub>x</sub> InSe	530.72	

### 3.2 Quantitative XPS of (0001) CS of Ni<sub>x</sub>InSe intercalates by the pure standards method

The pure standards method for the quantitative XPS is based on linear interpolation of the signal intensity of X-photoelectrons of a certain I<sub>E</sub><sup>i</sup>-th chemical element regarding its surface concentration in the studied object.

$$I_E^i \approx \alpha \times C_i, \quad (2)$$

where  $\alpha$  is the coefficient of linear interpolation. More precisely, this relationship can be written as

$$I_E^i \approx k \cdot I_{hv} \cdot \sigma_{ion}^i \cdot \lambda_{em.uap}^i \cdot C_i, \quad (3)$$

where  $k$  is the instrument coefficient or instrument function;  $I_{hv}$  is the X-radiation intensity;  $\sigma_{ion}^i$  is the effective ionization cross-section of atoms of the  $i$ -th type by quanta with energy  $h\nu$ ;  $\lambda_{em.uap}^i$  is the electron free path (electron escape depth) for their elastic scattering;  $C_i$  is the surface concentration of atoms of the  $i$ -th type of the studied material;  $S_i$  is the relative elemental sensitivity of the given instrument to atoms of the  $i$ -th type.

To calculate the relative surface concentrations of atoms of chemical elements, it is necessary to have the peak "intensities"  $I_E^i$  for the pure standards of chemical elements. That is, one should perform calibration of the spectrometer by using the standards – to determine the relative elemental sensitivities  $S_i$  or sensitivity of the XPS method to different chemical elements.

$S_i$  is the elemental sensitivity factor (the relative elemental sensitivity) is obtained, when a certain element is normalized to the reference peaks by intensity or area under its reference peak. Normalization to the peak of

chemical element fluorine F 1s, for which it is assumed that  $S_{F1s} = 1$ , is performed.

Since the effective ionization cross-section of atoms of the  $i$ -th type by quanta with energy  $\sigma_{ion}^i(h\nu)$  will be different for different elements, as well as the electron escape depth for their elastic scattering (without energy losses)  $\lambda_{em.uap}^i$ . In the general pure standards method for the calculation of the relative atomic concentrations of elements, it is assumed, according to the hypothesis (equation (2)), that

$$I_i \approx S_i \times C_i, \quad (4)$$

and the total relative atomic concentration in the studied material in relative units is equal to

$$\sum_{i=1}^n C_i = 1. \quad (5)$$

The quantitative elemental analysis of the material surface by the XPS method in relative units (percentages) is carried out measuring the amplitudes of the reference XPS peaks of chemical elements in the spectra of photoelectrons  $I_E^i$  or determining the area of these peaks in "the number of pulses per second in the energy interval of the reference peak – total energy half-height width of the peak". Then, with respect to formula (4)

$$C_i = \frac{I_i}{S_i}, \quad (6)$$

where  $S_i$  is the elemental sensitivity factor of the  $i$ -th element;  $I_i$  is the intensity of the XPS peak of the  $i$ -th chemical element. Taking into account (5), formula (6) can be rewritten as follows

$$C_i = \frac{I_i}{S_i} = \frac{I_i/S_i}{\sum_i C_i} = \frac{I_i/S_i}{\sum_{i=1}^n I_i/S_i}, \quad (7)$$

where  $n$  is the number of chemical elements registered in the XPS spectrum of the surface of the investigated material. The relative atomic concentrations  $C_i$  of chemical elements of (0001) CS of Ni<sub>x</sub>InSe intercalates and in a thin interface layer of (0001) CS of Ni<sub>x</sub>InSe with the presence of adsorbates are calculated using expression (7) and given in Table 2.

$I_E^i$  is the area under the peak,  $S_i$  is the elemental sensitivity factor of the XPS method, which for the atoms registered in the interface layers is present in brackets for elements: Se (0.853), In (4.359), Ni (2.67), C (0.287), O (0.78). The peak area of elements is counted from the background line. The results of the quantitative analysis by the pure standards method using the XPS spectra for "pure" (0001) CS of Ni<sub>x</sub>InSe and for (0001) CS\*\* of intercalates of the adsorbates formed by the interface coating – Ni<sub>x</sub>InSe(C,O), are given in Table 2.

Thus, as seen from the results of the quantitative XPS analysis of the elemental composition of (0001) CS of Ni<sub>x</sub>InSe intercalates (without taking into account the adsorbed oxygen and carbon) for all LC of intercalates with different nickel concentration ( $x = 0; 0.5; 0.75; 1.0$ ;

2.0 wt. %) in the initial synthesized  $\text{InSe} + x \text{ wt. \%}$  of Ni ( $x \leq 2.0\%$ ) alloys and the LC grown from them by the Bridgman-Stockbarger method and subjected intercalation, the maximum nickel concentration at (0001) CS and, correspondingly, in the interlayer gaps in the amount up to 7.67 wt. % is observed at 0.75 wt. % of Ni in the synthesized alloys. Similar restrictions on the entry of Ni to InSe LC during its growth were observed in [4].

#### 4. TOPOGRAPHY AND CRYSTALLOGRAPHY OF (0001) CS OF $\text{Ni}_x\text{InSe}$ INTERCALATES

The topography of (0001) CS obtained *ex situ* by cleaving  $\text{Ni}_x\text{InSe}$  LC intercalates was studied by the STM method, and the atomic structure and crystallography – by the LEED method.

The experiments with STM were conducted on the setup "Omicron NanoTechnology STM/AFM System", in the construction of which there is a conducting tungsten tip of the diameter of 500  $\mu\text{m}$ . The STM studies of the topography of (0001) CS of pure InSe and intercalated InSe(Ni) crystals were done in UHV ( $2 \times 10^{-10}$  torr) at 295 K in the mode of direct tunneling current. A special software WSxM v.4.0 developed by Nanotec Electronica (Spain, <http://www.nanotec.es>) is used for the processing of the STM data.

The experiments with LEED were carried out using vacuum module ErLEED 100 (Auger electron spectroscopy (AES) and LEED) by SPECS Surface Nano Analysis (<http://www.specs.de>), assembled on the header flange, which joins the UHV chamber, whose vacuum is equal to  $6 \times 10^{-10}$  torr. The electron gun used in LEED with

the cathode of LaB<sub>6</sub> single crystal provided the current strength of the electron beam of diameter up to 1 mm in the (0001) CS plane of the sample up to 1  $\mu\text{A}$  at the accelerating voltage up to 200 V, which is sufficient to obtain bright diffraction reflexes.

Using the surface-sensitive methods, such as STM and LEED, one can learn about both the two-dimensional structures and their parameters at CS, as well as their possible reconstruction, and also the nanostructures formed on them.

The electron-energy structure of CS of pure InSe and  $\text{Ni}_x\text{InS}$  intercalates was studied by the STS method.

The LEED studies started in ~60 min after cleaving *ex situ* and were carried out in the UHV chamber at  $P = 6 \times 10^{-10}$  torr and 295 K. Before studies, InSe samples were briefly warmed-up in the UHV chamber up to 200 °C in order to clean CS off adsorbed gases. A luminescent screen and recording with a digital video camera are used to visualize the LEED patterns. A special software SAFIRE Diffraction Image Acquisition and Processing System for LEED and RHEED v.15.5.15 developed by SPECS Surface Nano Analysis GmbH is utilized for the LEED data processing.

LEED images for reflection of (0001) CS of  $\text{Ni}_x\text{InSe}$  intercalates are illustrated in Fig. 6. LEED patterns for (0001) CS of  $\text{Ni}_x\text{InSe}$ , obtained at the bombarding electron energy in the range of  $E = 10\text{-}200$  eV, indicate the rhombohedral surface atomic structure and testify the structure perfection of InSe(Ni) (0001) CS in the minimal regions of coherence of the diffracted electron beam of ~ 0.1-1  $\mu\text{m}$ .

Table 2 – Quantitative analysis of (0001) CS of  $\text{Ni}_x\text{InSe}$  intercalates without and with\*\* accounting adsorbed oxygen and carbon

	Chemical element	Binding energy, eV	Half-height width of the peak, eV	Area under the peak, $I_E^i$ (pulses/sec)	Elemental sensitivity factor $S_i$ , rel. units	Atomic concentrations $C_i$ , %
CS	In 3d <sub>5/2</sub>	443.39	2.695	143453	4.359	61.43
	Se 3d <sub>5/2</sub>	53.70	2.669	14110	0.853	30.87
	Ni 2p <sub>3/2</sub>	856.47	2.839	10983	2.670	7.67
CS**	In 3d <sub>5/2</sub>	443.39	2.695	143453	4.359	11.36
	Se 3d <sub>5/2+3/2</sub>	51.85	2.669	14110	0.853	5.68
	Ni 2p <sub>3/2</sub>	856.47	2.839	10983	2.670	1.42
	C 1s	283.70	3.593	48748	0.278	60.50
	O 1s	530.72	3.097	47514	0.780	21.01

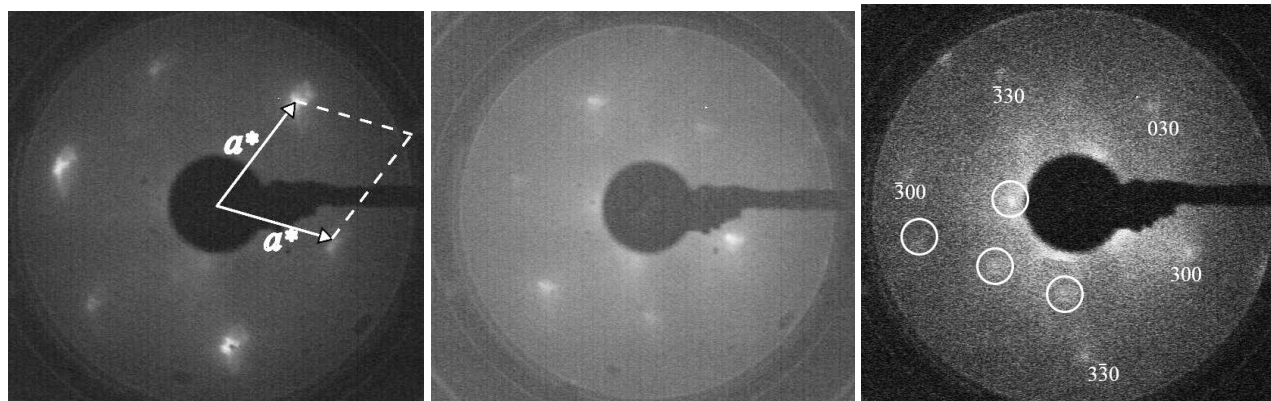


Fig. 6 – LEED images of (0001) CS of  $\text{Ni}_x\text{InSe}$  intercalates at different energies. a) 50 eV, b) 75 eV, c) 184.5 eV. In Fig.6a, arrows denote the vectors of the reciprocal surface lattice; in Fig. 6c, circles surround the reflexes of the nickel phase together with the "indexed" reflexes of (0001) CS of the third-order InSe

Clear reflexes of the 1-st, 2-nd, and 3-d orders are observed in the LEED patterns of (0001) CS of  $\text{Ni}_x\text{InSe}$  that was not always easily observed for the LEED patterns of (0001) CS of pure InSe. This is associated with the highest surface conductivity of the  $\text{Ni}_x\text{InSe}$  samples, on the surface of which nickel clusters are present. For pure, non-intercalated InSe LC, as the STM/STS results confirm, the additional impurity jumping conductivity over the "Mott states" is absent; therefore, their surface under irradiation by an electron gun of the LEED module is charged that leads to blurring of the LEED patterns of (0001) CS of pure InSe.

Change in the energy of low-energy electrons, which bombard the surface, and, thus, change in the length of the de Broglie electron wave and diffraction conditions and appearance of the interference reflexes leads to the change in the distances between the diffraction reflexes and their brightness (Fig. 6a, b).

The above conditions allowed to observe the two-dimensional structural phase of crystalline nickel at the interlayer (0001) CS of  $\text{Ni}_x\text{InSe}$  (Fig. 6c). These reflexes for the two-dimensional nickel phase are surrounded by circles. Not all reflexes of the two-dimensional Ni phase with a "square" structure are observed on the luminescent screen, since it is difficult to provide the conditions of coherence for the interference of diffracted de Broglie electron waves. Deformations and breaks of the individual elementary layers of the LC with possible change of the  $\gamma$ - to  $\beta$ - layer polytype, which we have observed in the work [15], take place at cleaving of InSe LC.

With increasing energy of primary electrons, there is a decrease in the intensity of reflexes, as if they were the tops of one of the "triangles", with simultaneous preservation/amplification of intensity for reflexes, which form another "triangular" (Fig. 6a).

These results, as well as those partially presented in our work [13], confirm that InSe crystals are characterized by a layered structure in the form of "sandwiches", in which two inner layers of In atoms are located between two outer layers of Se atoms; orientation of these four sublayers is perpendicular to the  $c$ -axis (see Fig. 1a and Fig. 7 (at the left)). Bonds inside the "sandwich" are the covalent ones and much stronger than the van der Waals bonds between adjacent "sandwiches", and, thus, such LC as InSe are easily cleaved along the outer plane of the "sandwich", which represented in our experiments the surface of the specified orientation – (0001)[16].

The values of the constants of the two-dimensional lattice, which has the rhombic structure in the plane of InSe (0001) CS, according to InSe crystallography (bulk rhombohedral lattice [9, 17, 18]) are equal  $a = b = 4.0 \text{ \AA}$  and correspond to the values, which are typical for the

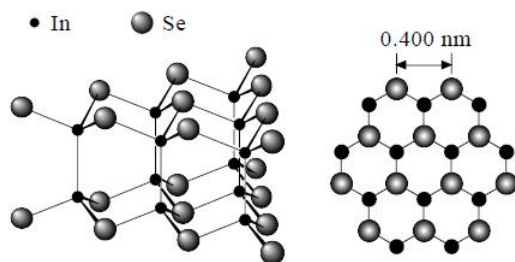


Fig. 7 – Structure of the  $\gamma$ -InSe crystal (at the left) and view of (0001) CS of InSe (at the right) [19]

bulk InSe crystal [9, 18, 19], that allows the entry of Ni atoms into the interlayer gap. The image of the atomic array in the two-dimensional InSe lattice and distances corresponding to the lattice constants are illustrated in Fig. 7 (at the right) [19].

That is, the crystal structure of InSe LC, where the distance between layers is equal to  $3.08 \text{ \AA}$  [20], allows to assume that nickel forms the phase when enters the interlayer gap with intercalation –  $\text{Ni}_x\text{InSe}$ . Additional reflexes on the LEED patterns of (0001) CS of  $\text{Ni}_x\text{InSe}$  intercalates corresponding to the two-dimensional phase of metal nickel at the interlayer (0001) CS are well observed for the energy of primary electrons of  $E \sim 170\text{-}200 \text{ eV}$  and are presented for the first time in our work [13]. The estimations of the two-dimensional lattice constants for Ni at the interlayer (0001) CS by the LEED patterns are equal to  $a = 3.4\text{-}3.5 \text{ \AA}$ . We remind that crystalline metal nickel has a cubic lattice with constants of  $a = 3.52 \text{ \AA}$ . The above considerations as for the ordering of Ni clusters into the two-dimensional metal phase at (0001) CS of  $\text{Ni}_x\text{InSe}$  intercalates are also confirmed by the results of the STM/STS studies. Calculation of the two-dimensional lattice constants  $a$  of InSe and Ni at (0001) CS of  $\text{Ni}_x\text{InSe}$  intercalates by the LEED results was carried out by the formula (8) with accounting the geometry of the LEED experiment.

$$a = \frac{2\pi}{\sin \theta (0,5123\sqrt{E})} n, \quad (8)$$

where  $E$  is the energy of incident electrons;  $\theta$  is the angle of scattered electrons, which give the diffraction-interference reflexes on the luminescent screen;  $n$  is the order of diffraction reflexes at the LEED pattern.

We should remind that with increasing energy of electrons incident on (0001) CS, the angle of scattered electrons  $\theta$  decreases. So, on the LEED patterns obtained in the energy range of  $10\text{-}200 \text{ eV}$  with increasing energy of incident electrons, one can observe a decrease in the distances between the reflexes (movement of the reflexes to the LEED pattern center) with increasing number of visible diffraction reflexes – appearance within view of a luminescent screen of the diffraction reflexes of higher orders without changing the symmetry of the location of the diffraction reflexes.

Theoretical model for the calculation of the surface lattice constants by the LEED patterns was proposed in the work [21], and its adequacy is confirmed in our works [22-24], in which the estimation of the two-dimensional lattice constants of (100) CS of  $\text{In}_4\text{Se}_3$  LC by the LEED results has been performed.

The study of the topography of (0001) CS of pure and intercalated with Ni InSe LC is conducted by the STM method and of the electron-energy structure and density of electronic surface states – by the STS method.

The results of STM of InSe(Ni) (0001) CS (Fig. 8a, b) indicate the unreconstructed structure of the InSe(Ni) LC surface, which is similar to the surface of pure InSe LC and coated with clusters of intercalate (nickel) in the form of nanoscale spots. Application of the software 2D FFT filtering to these clusters, in order to detect periodicity in the image (Fig. 8c), demonstrates the structure with a period close to  $3.5 \text{ \AA}$  (Fig. 8d, e), which is typical for the two-dimensional surface lattice of metal nickel located at (0001) CS of  $\text{Ni}_x\text{InSe}$  intercalates.

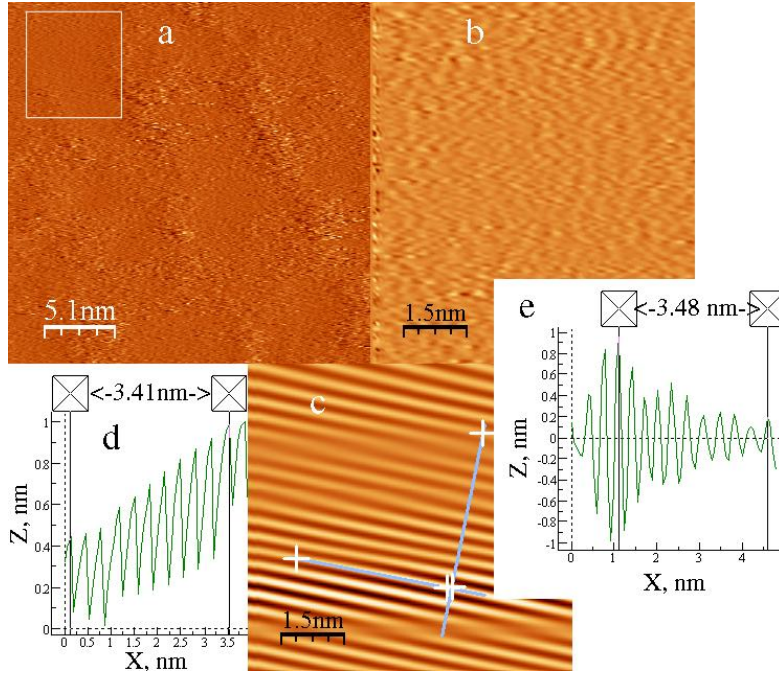


Fig. 8 – Topography of (0001) CS of  $Ni_xInSe$  intercalates. a) 2D STM image of the part of CS with the size of  $26 \times 26 \text{ nm}^2$  obtained in the mode of direct tunneling current of 103 pA and bias voltage of 4.6 V. b) Magnified fragment of the surface in the form of a rectangle from the upper left angle in the image (a) of the size of  $7.3 \times 8.1 \text{ nm}^2$ . c) 2D FFT-filtered image of the fragment (b) of (0001) CS of  $Ni_xInSe$  intercalate and its profiling in two mutually perpendicular directions: d) profile of a periodic structure of (0001) CS along the corrugation ridge; e) profile of a periodic structure of (0001) CS perpendicular to the corrugation ridge

Periodic distances along the profile (d) and profile (e) in Fig. 8 for better visualization are taken in both cases for ten periodicities, i.e. ten lattice constants  $10 \times a$  – depicted periodicities (see profiles). The measured distances are written between markers, and for Fig. 8d the distance of  $10 \times a$  is equal to 3.41 nm and for Fig. 8e – 3.48 nm; and in both cases they coincide well with the constant of two-dimensional nickel lattice in the interlayer gap of  $Ni_xInSe$  intercalate, i.e. at its (0001) CS. These values of the constants of two-dimensional square lattice  $a = 3.41 \text{ \AA}$  and  $3.48 \text{ \AA}$  at (0001) CS of  $Ni_xInSe$  intercalate satisfactorily correspond to the cubic lattice constant of metal nickel, which is equal to  $3.52 \text{ \AA}$ .

Thus, the STM results also confirm: firstly, the nickel arrangement in the interlayer cleavage gap of  $Ni_xInSe$  intercalate; secondly, the absence of interactions of nickel atoms with indium and selenium ones and formation of own two-dimensional phase of metal nickel at (0001) CS of  $Ni_xInSe$  intercalate.

Application of STS for obtaining the electron-energy structure of (0001) CS of  $Ni_xInSe$  intercalate and analyzing the density of electronic states at (0001) CS confirmed the presence of Ni at (0001) CS of  $Ni_xInSe$  intercalate in a free state unbounded with InSe (Fig. 9).

The tunneling current between the tip and CS of the sample can be presented as [25]

$$I_t \propto \exp(-\alpha S\sqrt{\Phi}) \times \int_0^{eV} N_s(E) \times N_t(eV - E) dE, \quad (9)$$

where  $\alpha = 2\sqrt{2m}/\hbar$ ,  $S$  is the tunneling interval,  $\Phi$  is the tip work function,  $E$  is the electron energy with respect to the Fermi level;  $N_s(E)$  is the local density of surface electronic states of CS under the tip, and  $N_t = \text{const}$  at the end of the tip.

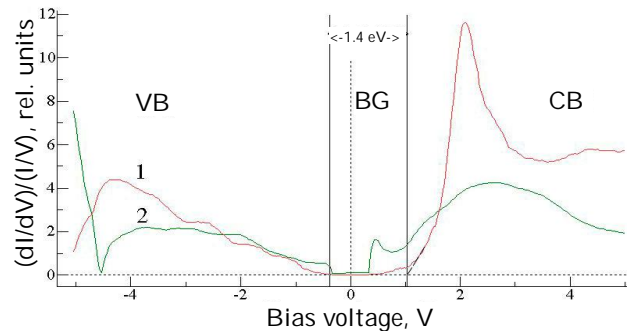


Fig. 9 – Results of STS of (0001) CS of pure InSe (curve 1) and  $Ni_xInSe$  intercalate (curve 2) illustrated by differentiated and normalized curves  $(dI/dV)/(I/V)$ , which represent the energy dependences of the local density of surface electronic states  $N_s(E)$  and demonstrate the electron-energy structure of (0001) CS: VB – valence band; BG – band gap; CB – conduction band

Curve  $dI_t(V)/dV \propto (dI/dV)/(I/V)$  of the dependence as a function of bias voltage  $V$  is a function of energy ( $eV = E$ ) and proportional to the local density of surface electronic states  $N_s(E)$  of (0001) CS [25]. According to equation (9)

$$dI_t / dV \propto N_s(E). \quad (10)$$

Curves 1 and 2 (Fig. 9) are characteristic for different points chosen on the area of  $50 \times 50 \text{ nm}^2$  of (0001) CS and are a result of their integration at the specified area. Curve 1 of the local density of surface electronic states of (0001) CS of InSe LC demonstrates typical (for pure InSe) band gap (BG) of the value of 1.4 eV. Curve 2 for (0001) CS of  $Ni_xInSe$  intercalates demonstrates the presence of the density of local states of pure InSe energetically located in the BG due to the metal component (Ni) at the cleavage surface.

According to the STS method [25], curve 2 is a differentiated-normalized sum of the local densities of surface states of (0001) CS of pure InSe and  $\text{Ni}_x\text{InSe}$  intercalate intercalated with Ni, where in the band of forbidden energies of InSe LC there are scattered Mott states with different depth of occurrence caused by unbounded with InSe Ni at (0001) CS of  $\text{Ni}_x\text{InSe}$  intercalate.

## 5. CONCLUSIONS

1. The intense peaks of chemical elements of the main InSe phases – the doublet peaks of selenium Se  $3d_{5/2+3/2}$  and indium In  $3d_{3/2+5/2}$  and intercalating Ni impurities Ni  $2p_{3/2}$  for  $\text{Ni}_x\text{InSe}$  intercalates – are revealed in the XPS spectra by XPS studies of (0001) CS of InSe LC and their  $\text{Ni}_x\text{InSe}$  intercalates. Moreover, it is established the presence at (0001) CS of O 1s, N 1s, C 1s peaks, which naturally appear due to the adsorption of the laboratory atmosphere gases  $\text{N}_2$ ,  $\text{O}_2$ ,  $\text{CO}_2$ , CO,  $\text{H}_2\text{O}$ , and  $\text{CH}_x$  when cleaving crystals in air before displacement of the samples into the analytical spectrometer chamber.

2. As the decompositions of the reference peaks of Ni Ni  $2p_{3/2}$ , oxygen O 1s, carbon C 1s and the analysis of the doublet peaks of selenium Se  $3d_{5/2+3/2}$  and indium In  $3d_{3/2+5/2}$  showed, nickel, which is located in the interlayer gaps of  $\text{Ni}_x\text{InSe}$  intercalates ( $x = 0; 0.5; 0.75; 1.0; 2.0$  wt. %) and, correspondingly, at the interlayer (0001) CS, does not interact with selenium, indium, interactions with oxygen and carbon are absent, and it represents, in a greater extent, a finely dispersed phase of metal nickel clusters in the interlayer gaps of  $\text{Ni}_x\text{InSe}$ .

3. The relative atomic concentrations of chemical elements at (0001) CS of  $\text{Ni}_x\text{InSe}$  intercalates ( $x = 0; 0.5; 0.75; 1.0; 2.0$  wt. %) with and without taking into account adsorbed gases are calculated using the quantitative XPS technique by the pure standards method.

4. It is established that for LC intercalates with different nickel concentration in the initial synthesized alloys

InSe +  $x$  wt. % of Ni ( $x \leq 2.0$  %) and LC grown from them by the Bridgman-Stockbarger method and subjected intercalation, the maximum Ni concentration at (0001) CS of  $\text{Ni}_x\text{InSe}$  intercalates and, correspondingly, in the interlayer gaps in the amount up to 7.67 wt. % is observed for 0.75 wt. % of Ni in the alloys that confirms its shift into the interlayer gaps in the intercalation.

5. In the LEED patterns of  $\text{Ni}_x\text{InSe}$  intercalates one observes clear reflexes of the 1<sup>st</sup>, 2<sup>nd</sup> and 3<sup>d</sup> orders, whose sequence of occurrence is synchronized with an increase in the energy of bombarding electrons. The above is not always observed for the LEED patterns of pure InSe and is caused by higher surface conductivity and structural stability of (0001) CS of  $\text{Ni}_x\text{InSe}$  intercalates.

6. Appearance of additional LEED reflexes, which correspond to the phase of metal Ni clusters at (0001) CS of  $\text{Ni}_x\text{InSe}$  intercalates, depends on the structural perfection of (0001) CS and, correspondingly, the energies of bombarding electrons and fulfillment of the conditions of coherence of electron diffraction and interference.

7. The two-dimensional lattice constants of (0001) CS for both pure InSe and  $\text{Ni}_x\text{InSe}$  intercalates, calculated on the basis of the LEED images, correspond to the values typical for the InSe crystal volume of  $a = b = 4.0$  Å that indicates the structural stability of (0001) CS.

8. The STM studies of (0001) CS of  $\text{Ni}_x\text{InSe}$  intercalates allow to conclude the absence of reconstruction in the structure of (0001) CS of  $\text{Ni}_x\text{InSe}$  LC as well as the surface of pure InSe LC. STM also confirms the presence in the interlayer gaps of the local areas of nickel with the surface lattice which corresponds to the projection on (0001) CS of  $\text{Ni}_x\text{InSe}$  intercalates of the cubic structure of metal nickel with the period of 3.5 Å.

9. Based on the results of STS studies, it is established the presence of the localized surface states in the BG of  $\text{Ni}_x\text{InSe}$  intercalates caused by metal Ni phase at their (0001) CS in contrast to pure InSe.

## REFERENCES

- I.I. Grygorchak, *Phys. Chem. Solid State* 2 No 1, 7 (2001).
- B.P. Zakharchenya, V.L. Korenev, *Phys.-Usp.* 48, 603 (2005).
- S.A. Voytovych, I.I. Hryhorchak, O.I. Aksimentyeva, M.M. Mitsov, *Fizychna inzheneriya poverkhni* 5 No 3-4, 222 (2007).
- I.M. Stakhira, N.K. Tovstyuk, V.L. Fomenko, V.M. Tsmots, A.N. Shchupliak, *Semiconductors* 45, 1258 (2011).
- A. Fert, *Phys.-Usp.* 51, 1336 (2008).
- Yu.P. Sukhorukov, B.A. Gizhevskii, E.V. Mostovshchikova, A.Ye. Yermakov, S.N. Tugushev, E.A. Kozlov, *Tech. Phys. Lett.* 32 No 2, 132 (2006).
- Ya.M. Buzhuk, L.S. Demkiv, Y.M. Stakhira, N.K. Tovstyuk, V.L. Fomenko, *Novi Tekhnolohiyi* 2 No 28, 68 (2010).
- Z.R. Kudrynskyi, *Formuvannya ta vlastyosti nanostruktur na osnovi sharuvatykh krystaliv selenidiv indiyu i haliyu*. Avtoref. dys. kand. fiz.-mat. nauk (Chernivtsi: 2014).
- J.F. Sanchez-Royo, G. Munoz-Matutano, M. Brotons-Gisbert, J.P. Martinez-Pastor et al., *Nano Res.* 7 No 10, 1556 (2014).
- P. Galiy, A. Musyanovych, *Functional Mater.* 12 No 3, 467 (2005).
- P.V. Galiy, A.V. Musyanovych, T.M. Nenchuk, *J. Electr. Spectr. Rel. Phenom.* 142 No 2, 121 (2005).
- NIST X-ray Photoelectron Spectroscopy Database, NIST Standard Reference Database 20, Ver. 4.1, Distributed by the Measurement Services Division of the National Inst. of Stand. and Techn. (NIST), <http://srdata.nist.gov/xps/>.
- P.V. Galiy, Ya.B. Losovyj, T.M. Nenchuk, A. Ciszewski, P. Mazur, I.R. Yarovets, *The XXth International Seminar on Physics and Chemistry of Solids*, 49 (Lviv: 2015).
- P. Galiy, T. Nenchuk, *Visn. Lviv. un., Ser. fiz.* 32, 121 (1999).
- P. Galiy, T. Nenchuk, A. Ciszewski, P. Mazur, S. Zuber, I. Yarovets, *Metallofiz. Nov. Tekhnol.* 37 No 6, 789 (2015).
- L.I. Man, R.M. Imamov, S.A. Semiletov, *Kristallografiya* 21 No 3, 628 (1976).
- J. Rigoult, A. Rimskeya, A. Kuhn, *Acta Crystallographica Section B* 36 No 4, 916 (1980).
- D.M. Bercha, K.Z. Rushchanskii, L.Yu. Kharkhalis, M. Sznajder, *Condens. Matter Phys.* 3 No 4, 749 (2000).
- T. Hayashi, K. Ueno, K. Saiki, A. Koma, *J. Crystal Growth* 219 No 1-2, 115 (2000).
- Hydrogen Storage* (Ed. by J. Liu) (InTech: 2012).
- Erica T. Shen, Nancy Yu, Dr. Kenneth T. Park, Low-energy electron diffraction and ultraviolet photoemission spectroscopy study of  $(1 \times 1)$   $\text{TiO}_2$  (110). CASPER Summers – Research Experience for Undergraduates (REU) Program, 2009 REU Final Projects. Baylor Univer., Waco, USA. – 2009, 7 p. <http://www.baylor.edu/content/sevices/document.php/98314.pdf>.
- P.V. Galiy, T.M. Nenchuk, I.R. Yarovets, *J. Nano-Electron. Phys.* 6 No 2, 02029 (2014).
- P.V. Galiy, *Khimiya, fizyka ta tekhnolohiya poverkhni* 5 No 3, 245 (2014).
- P.V. Galiy, Ya.B. Losovyj, T.M. Nenchuk, I.R. Yarovets, *Ukr. J. Phys.* 59 No 6, 612 (2014).
- P. Galiy, T. Nenchuk, O. Dveriy, A. Ciszewski, P. Mazur, S. Zuber, *Visn. Lviv. un., Ser. fiz.* 43, 28 (2009).